

# The fluorescence properties and binding mechanism of SYTOX green, a bright, low photo-damage DNA intercalating agent

Shreyasi Thakur<sup>1,2,3</sup> · Diego I. Cattoni<sup>1,2,3</sup> · Marcelo Nöllmann<sup>1,2,3</sup>

Received: 16 December 2014 / Revised: 5 April 2015 / Accepted: 8 April 2015 / Published online: 31 May 2015  
© European Biophysical Societies' Association 2015

**Abstract** DNA intercalators are widely used in cancer therapeutics, to probe protein–DNA interactions and to investigate the statistical–mechanical properties of DNA. Here, we employ single-molecule fluorescence microscopy, magnetic tweezers, and ensemble-binding assays to investigate the fluorescence properties and binding mechanism of SYTOX green, a DNA labeling dye previously used for staining dead cells and becoming of common use for single-molecule methodologies. Specifically, we show that SYTOX green presents several advantages with respect to other dyes: (1) binds DNA rapidly and with high affinity; (2) has a good signal-to-noise ratio even at low concentrations; (3) exhibits a low photobleaching rate; and (4) induces lower light-induced DNA degradation. Finally, we show that SYTOX green is a DNA intercalator that binds DNA cooperatively with a binding site of 3.5 bp, increasing the DNA length upon binding by 43 %, while not affecting its mechanical properties.

**Keywords** DNA intercalator · DNA staining · Single molecule · Intercalators binding mechanism · Fluorescence microscopy

**Electronic supplementary material** The online version of this article (doi:10.1007/s00249-015-1027-8) contains supplementary material, which is available to authorized users.

✉ Marcelo Nöllmann  
marcelo.nollmann@cbs.cnrs.fr

<sup>1</sup> Centre National de la Recherche Scientifique, Unité Mixte de Recherche 5048, Centre de Biochimie Structurale, 29 rue de Navacelles, 34090 Montpellier, France

<sup>2</sup> Institut National de la Santé et la Recherche Médicale, Unité 1054, Montpellier, France

<sup>3</sup> Université de Montpellier, Montpellier, France

## Introduction

Single-molecule microscopy is a rapidly evolving ensemble of methods that provide key information on the dynamic behavior, kinetics, and heterogeneity of proteins and molecular motors involved in the organization, segregation, replication, repair, and transcription of DNA (Amitani et al. 2006; Bianco et al. 2001; Blainey et al. 2006; Loparo et al. 2011; van Mameren et al. 2008). Probing DNA–protein interactions in single-molecule experiments often require both manipulation and visualization of DNA and protein through direct labeling with fluorescent compounds. The two most frequently used approaches to simultaneously visualize DNA and protein are optical tweezers coupled with fluorescence microscopy and TIRFM (total internal reflection fluorescence microscopy) (van Mameren et al. 2008). In both cases, DNA is visualized by the use of DNA staining dyes that exhibit enhanced fluorescence upon binding. The most common mode of interaction of these dyes with DNA is intercalation: a binding mode in which small molecules insert their planar aromatic moiety between two adjacent base pairs (bp) of double-stranded DNA (dsDNA) (Lerman 1961). The study of the changes in DNA structural and mechanical properties induced upon intercalation of small molecules is important as these complexes can dramatically influence the binding, activity, and movement of enzymes on DNA. Additionally, intercalating fluorescent dyes can produce light-induced chemical modifications in DNA, such as the introduction of single-strand and double-strand breaks (ssb and dsb, respectively, e.g., Akerman and Tuite 1996; Colmenarejo et al. 1995; Yu et al. 2009). Furthermore, because of their specific property of interfering with DNA–protein interactions, intercalators (e.g., proflavin) are used in anticancer drug formulations. Thus, understanding the binding modes, intercalation kinetics, and

light-induced damage of DNA by intercalating agents is of utmost importance in the development of more specific and efficient dye molecules and drugs (Hurley 2002).

Monomeric and dimeric dyes are widely used in single-molecule fluorescence imaging of DNA. Monomeric intercalating dyes, such as ethidium bromide or YO-1, have a moderate binding affinity for dsDNA, typically in the  $\mu\text{M}$  range (Petty et al. 2000). In contrast, dimeric bis-intercalators such as YOYO-1 exhibit a higher DNA binding affinity [ $\sim 5\text{--}50$  nM, depending on ionic strength (Günther et al. 2010; Gurrieri et al. 1997; Petty et al. 2000)] and display a  $\sim 1000$ -fold increase in fluorescence intensity upon binding dsDNA, making it the most commonly used dye for single-molecule DNA-imaging applications. Its application, however, requires specific strategies, not always fully compatible with optimal experimental conditions. On the one hand, YOYO-1 requires long incubation times and high temperatures ( $>1$  h at  $50^\circ\text{C}$ ) to obtain homogeneous DNA staining patterns (Carlsson et al. 1995) and binds rather slowly to DNA at the single-DNA molecule level  $\sim 5$  min for 40 nM YOYO-1 under TIRFM conditions (Reuter and Dryden 2010). On the other hand, the excitation of YOYO-1 can lead to the production of reactive oxygen species and free radicals that can cleave the DNA phosphate chain triggering single-strand breaks which, upon accumulation, lead to double-strand breaks (Akerman and Tuite 1996; Cadet et al. 2003). To mitigate this problem, the DNA base pair-to-dye ratio can be reduced, but this degrades the fluorescent signal and the localization precision. Alternatively, scavengers of reactive oxygen species (ROS) can be employed, but these can reduce the pH in the vicinity of DNA, which could affect specific protein–DNA interactions.

SYTOX are a family of nucleic acid staining dyes commonly used as dead-cells markers that have only recently been used for single-cell and single-molecule experiments (Blainey et al. 2006; Hamdan et al. 2009; Ptacin et al. 2008; Tanner et al. 2009). SYTOX dyes exhibit a large ( $>1000$ -fold) fluorescence enhancement upon DNA binding, have a high DNA binding affinity (as reported by its manufacturers), show little base selectivity, and exist in different colors spanning the whole visible spectrum. Previous studies have shown that SYTOX green fluorescence increases significantly also when bound to single-stranded DNA, although fluorescence enhancement is much lower than when bound to dsDNA (Roth et al. 1997). It was previously suggested that SYTOX are monomeric dyes (Yan et al. 2000), although their exact molecular structure is proprietary information of Molecular Probes (Thermo Fisher Scientific, OR, USA). Here, we employ TIRFM, magnetic tweezers, and equilibrium binding to characterize the use of SYTOX green as a DNA agent for single-molecule studies and to investigate its DNA binding mechanism.

## Materials and methods

### Preparation of DNA samples

For TIRFM experiments, biotin-labeled  $\lambda$ -DNA was prepared by ligating the 12 base pairs cos overhangs of linearized  $\lambda$ -DNA (New England Biolabs, Ipswich, USA; at a concentration of  $8 \times 10^{-10}$  M) with 5'-biotin-modified oligo1 (5'-AGGTCGCCGCC-Biotin-3';  $8 \times 10^{-9}$  M; Eurogentec, Seraing, Belgium) using T4 DNA Ligase (New England Biolabs, Ipswich, USA).

For magnetic tweezers experiments, 14.7-kb DNA fragments were used. Short DNA linker fragments ( $\sim 500$  bp) possessing either biotinylated or digoxigenated dUTP were generated by PCR as described (Stone et al. 2003), digested with *Bam*HI and *Xho*I, and specifically ligated to the 14.7 kb *Bam*HI/*Sal*I digestion product of the pPIA6 plasmid. All other chemicals used in this work were of analytical grade.

### Construction of micro-fluidics chambers and TIRFM setup

Coverslips were cleaned by using a plasma cleaner (Diener Electronics, Jettingen, Germany) and functionalized with aminosilane (AbCys Laboratories, Cortaboef, France) resulting in a surface with reactive amine groups. To avoid non-specific DNA sticking, the functionalized surface was passivated by treatment with a mixture of biotinylated and non-biotinylated polyethylene glycol (PEG, Abcys Laboratories, Cortaboef, France).

The flow chamber was built by drilling two holes on the opposite ends of a clean coverslip using a  $\text{CO}_2$  laser cutter (Thermoflan, Le Vigan, France). The flow chamber was assembled by putting together a drilled coverslip, a PEG-functionalized coverslip, and a parafilm spacer ( $\sim 100$   $\mu\text{m}$  thickness). The spacer was then sandwiched between the two coverslips and sealed by heating on a heat block at  $95^\circ\text{C}$ , creating a single channel in the middle with two holes at the opposite ends. Polyethylene tubes (PE50, Harvard Apparatus, Holliston, USA) were connected to the holes through homemade adaptors. Buffer and samples were injected into the chamber through a syringe pump (Harvard Apparatus, Holliston, USA).

A homemade TIRF setup based on a Zeiss Axiovert 100 inverted microscope equipped with a Plan Fluor 100X/1.45 NA objective (Zeiss, Le Peck, France) was used. The 488-nm line of an argon laser was used to excite YOYO-1 (Molecular Probes, Thermo Fisher Scientific, OR, USA) and SYTOX green (Molecular Probes) and their fluorescence signal collected through the same objective, passed through a  $525 \pm 25$ -nm emission filter (Chroma, VT, USA) and imaged onto an EM-CCD camera (Andor iXon,

DU888, Belfast, Ireland). The laser power was controlled by an acoustic-optic modulator. The camera exposure time used was 100 ms in all cases at a gain of 300.

### DNA imaging and processing

The flow chamber functionalized with biotin and PEG was incubated with 0.2 mg/ml streptavidin (Invitrogen, Thermo Fisher Scientific) for 10 min, and excess streptavidin washed out with TE buffer (20 mM Tris pH 7.5, 0.1 mM EDTA). Biotin-labeled  $\lambda$ -DNA was loaded at a concentration of 1 pM into the chamber in TE buffer at a flow rate of  $\sim 50$   $\mu$ l/min and incubated for 15 min to allow the formation of DNA attachments through biotin–streptavidin interactions. Unbound DNA was washed out the chamber by flowing 500  $\mu$ l of degassed DNA imaging buffer (13 % sucrose, 40 mM NaHCO<sub>3</sub>, 50 mM Tris pH 7.5, 15 mM dithiothreitol) at a flow velocity of  $\sim 100$   $\mu$ l/min. This buffer is typically used for visualization of DNA when using intercalating dyes, see for example (Reuter and Dryden 2010). For all experiments,  $\lambda$ -DNA was flow stretched at a flow velocity of 100  $\mu$ l/min. Signal-to-noise ratios (SNR) were calculated as  $SNR = (I_{DNA} - I_{background}) / I_{noise}$ , where  $I_{DNA}$  is the fluorescence signal on the DNA,  $I_{background}$  is the background intensity baseline (measured as the intensity on the background, i.e., where no DNA is present), and  $I_{noise}$  is the standard deviation of the background signal and represents the noise level of the measurement.

For SYTOX green experiments,  $\lambda$ -DNA was first tethered to the surface and imaging buffer with different SYTOX green concentrations was added a posteriori. Due to the slow reported binding kinetics of YOYO-1 by gel-electrophoresis (Carlsson et al. 1995),  $\lambda$ -DNA was first incubated for  $\sim 120$  min outside the observation chamber at the desired YOYO-1 concentration, then introduced into the micro-fluidics chamber, allowed to bind to the surface, and stretched by flow with a solution having the same concentration of dye as that used for the incubation.

Kymographs were constructed from movies of dye-stained single DNA molecules by applying the ImageJ plugin ‘MultipleKymograph’ ([http://www.embl.de/eamnet/html/body\\_kymograph.html](http://www.embl.de/eamnet/html/body_kymograph.html)) with a line thickness of three pixels. Intensity vs. time traces were obtained by drawing a region of interest (ROI) around single DNA molecules (which contained as little background as possible) and integrating the total fluorescence signal in each frame. For each movie, the background was estimated by the same procedure with a similar sized-ROI placed on the background nearby the DNA molecule.

The cumulative probability of producing dsb was calculated by: (1) determining the times at which each single DNA molecule was breaking in a single field of view, (2) calculating the cumulative sum of broken DNA molecules

vs. time, (3) dividing the cumulative sum by the total number of DNA molecules in the field of view (often, for SYTOX green samples, not all molecules were broken) to obtain that cumulative probability. The number of molecules broken per unit time in a field of view ( $n_{i,b}$ ) was estimated by the slope of the cumulative sum. The mean number of molecules broken per unit time ( $n_b$ ) was calculated by the averaging  $n_{i,b}$  over several fields of view (5–7, each containing 20–30 DNA molecules).

### Magnetic tweezers experiments

The magnetic tweezers setup consists of an inverted microscope (AxioObserver, Zeiss, Germany) equipped with a Plan Fluor 100 $\times$ /1.45 NA objective (Zeiss, Le Peck, France) mounted on a closed-loop piezoelectric stage (NanoF100, MCL, Madison, WI, USA) with nanometer resolution. Permanent magnets (custom made) are mounted on a fast, sub-micron-resolution motorized stage (PI, Karlsruhe, Germany). The flow cell was mounted on an  $x$ – $y$  motorized stage (ASI, Eugene, OR, USA). Imaging was performed with an EM-CCD camera (Ixon, Andor, Belfast, Ireland). Camera exposure time was 1 ms. Data were acquired and analyzed by using homemade software written in Labview (National Instruments; Austin, TX) (Nollmann et al. 2007). Dynamic changes in DNA extension were measured in real time at 50 Hz by comparing the bead diffraction ring pattern with a previously calibrated set of images taken at known focal displacements. To ensure accuracy of our extension measurements, each experimental setup was individually calibrated by an automated routine.

An uncoated microfluidics chamber was incubated with 5 mg/ml biotin-BSA (Sigma-Aldrich, St Louis, MO, USA) for  $\sim 2$  h, then washed with an excess of phosphate saline buffer (PBS, over 1 ml) and incubated with 0.2 mg/ml streptavidin for  $\sim 10$  min. Biotin and DIG labeled 14.7-kb DNA (Nollmann et al. 2007) was incubated with anti-DIG-functionalized magnetic beads of 1  $\mu$ m (My One Beads, Dynabeads, Thermo Fisher Scientific) in binding buffer (10 mM Tris pH 7.5, 500 mM NaCl, 1 mg/ml BSA) for 20 min to allow bead attachment at one end of the DNA. DNA-incubated beads were loaded into the fluidics chamber at 50  $\mu$ l/min and allowed to incubate for 20 min to enable DNA attachments. Unbound beads were washed out of the chamber by passing  $\sim 1$  ml of binding buffer at a flow velocity of 100  $\mu$ l/min. The chamber was then flushed with running buffer (10 mM Tris pH 7.5, 20 mM NaCl, 1 mg/ml BSA) containing SYTOX green at 1  $\mu$ M concentration.

To quantify the changes in elastic properties of DNA upon dye binding, we fitted the experimental force-extension curves to the worm-like chain model (WLC) (Marko and Siggia 1994) (Table 1):

**Table 1** List of symbols employed in this work

Symbol or abbreviated name	Extended name	Physical meaning	Units
$k_{\text{app}}$	Apparent association rate constant	Association rate of SYTOX green to DNA. $k_{\text{app}}$ depends on the ‘effective’ association rate constant ( $k_{\text{on}}$ ), ligand concentration and dissociation rate constant ( $k_{\text{off}}$ ). Experimentally, ligand concentrations and temporal resolution are chosen to favor the conditions in which $k_{\text{app}}$ will reflect closely $k_{\text{on}}$	$1 \text{ s}^{-1} \text{ M}^{-1}$
$\langle n \rangle$	Average number of occupied binding sites	Number of dye molecules per base pair	–
$K_{\text{Sytox}}^{\text{HH}}$	Apparent association constant	Apparent association constant for the SYTOX green–DNA complex as defined in the Hill model	M
$n_{\text{H}}$	Hill coefficient	Empirical coefficient that takes into accounts the non-hyperbolic behavior in binding isotherms (conventionally referred as cooperative behavior)	–
$N$	–	Represents the number of SYTOX green binding sites per base pair	–
$K_{\text{s}}$	Intrinsic binding constant	Intrinsic binding constant of SYTOX green for DNA as defined in the McGhee and von Hippel model	$\text{M}^{-1}$
$w$	–	Cooperativity parameter that specifies the relative affinity of an incoming ligand for a contiguous occupied site as opposed to an isolated binding site as defined in the McGhee and von Hippel model	–
$F$	External force	Force applied on DNA in magnetic tweezers experiments, calculated from the measurement of DNA extension and the mean square displacement of the magnetic bead particle	pN
$L_{\text{p}}$	Persistence length	Mechanical property quantifying the stiffness of a polymer (e.g., for DNA in vitro $L_{\text{p}} \sim 50 \text{ nm}$ )	nm
$L_0$	End-to-end distance of DNA	Contour length of DNA	nm

$$F = \frac{K_{\text{B}}T}{L_{\text{p}}} \left( \frac{1}{4} \frac{1}{\left(1 - \frac{x}{L_0}\right)^2} - \frac{1}{4} + \frac{x}{L_0} \right) \quad (\text{M1})$$

where  $F$  is the external force,  $x$  the extension,  $L_0$  the end-to-end distance (contour length), and  $L_{\text{p}}$  the persistence length.

Mean persistence length values and standard error for bare DNA and SYTOX green bound DNA were obtained from a least ten single DNA molecules in independent measurements.

### SYTOX green equilibrium binding

SYTOX green and  $\lambda$ -DNA were dissolved and diluted in the same buffer used for TIRFM experiments.  $\lambda$ -DNA and SYTOX green concentrations were determined by measuring light absorption at 260 and 504 nm, respectively, using an absorbance unit ( $A_{260}$ ) of  $50 \mu\text{g ml}^{-1}$  for  $\lambda$ -DNA and a molar extinction coefficient ( $\epsilon_{504}$ ) of  $6.7 \times 10^3 \text{ M}^{-1} \text{ cm}^{-1}$  for SYTOX green. The binding equilibrium at 25 °C was studied by fluorescence emission of SYTOX green at 530 nm following excitation at 488 nm as a function of increasing SYTOX green concentrations (1–1.4  $\mu\text{M}$ ) and constant DNA concentration (250 nM in bp). The fluorescence of these samples ( $F_{\text{b}}$ ) and reference samples,

prepared using the same SYTOX green concentrations but with a 100-fold excess of DNA ( $F_0$ ) were registered. Since the quantum yield of free SYTOX green in buffer is negligible and assuming that in a 100-fold DNA excess all the dye is bound, the average number of occupied binding sites (dye molecules per base pair),  $\langle n \rangle$ , and the concentration of free SYTOX green,  $[\text{Sytox}]_{\text{f}}$ , can be calculated according to Daniel and Weber (Daniel and Weber 1966):

$$\langle n \rangle = \frac{F_{\text{b}} [\text{Sytox}]_{\text{T}}}{F_0 [\text{bp}]_{\text{T}}} \quad (\text{M2})$$

$$[\text{Sytox}]_{\text{f}} = [\text{Sytox}]_{\text{T}} \left( 1 - \frac{F_{\text{b}}}{F_0} \right) \quad (\text{M3})$$

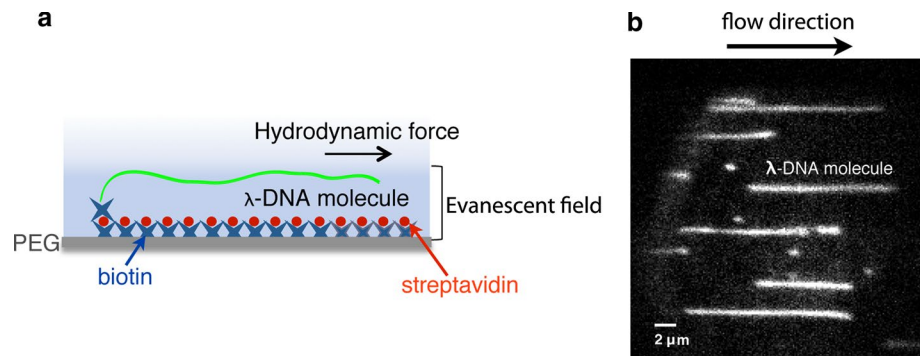
where  $[\text{Sytox}]_{\text{T}}$  and  $[\text{bp}]_{\text{T}}$  correspond to the total concentration of SYTOX green and base pairs of DNA, respectively.

## Results

### SYTOX green displays rapid DNA binding kinetics and slow light-induced photobleaching

To characterize the mechanism of DNA binding by SYTOX green and quantify its properties as a DNA staining agent for single-molecule experiments, we immobilized

**Fig. 1** **a** TIRFM experimental design. Individual biotin-labeled  $\lambda$ -DNA molecules were immobilized in the PEGylated surface of a microfluidics chamber and stretched by using flow force. SYTOX green/YOYO-1 were excited at 488 nm by TIRF illumination. **b** Example of a typical field of view of  $\lambda$ -DNA stained with SYTOX green



the biotin-labeled 5'-end of single  $\lambda$ -DNA molecules on a PEGylated surface and stretched them by using flow force in a custom-made micro-fluidics chamber (Fig. 1a). SYTOX green/YOYO-1 were excited by the 488-nm line of an Ar-laser by TIRF illumination and fluorescence emission was detected by wide-field imaging on a sensitive emCCD camera (Fig. 1b). First, we characterized the DNA binding kinetics of SYTOX green by continuously monitoring the increase of fluorescence signal of unstained, surface-tethered  $\lambda$ -DNA molecules upon addition of a low concentration of SYTOX green (10 nM in imaging buffer). Real-time imaging of single DNA molecules shows a lag phase followed by rapid increase in fluorescence signal that saturates after  $\sim 50$  s (Fig. 2a). Longer incubation times did not lead to any further increase in fluorescence (data not shown). From these images, the mean fluorescence signal per DNA molecule was calculated as a function of time (see “Materials and methods”). Figure 2b shows a typical fluorescence time-course with two well-defined phases. The first and slower phase corresponds to the arrival of dye after injection and may be affected by dye diffusion at the buffer barrier, incomplete mixing close to the surface, and initial dye depletion due to non-specific adsorption (lag time in Fig. 2b). We assume that binding of SYTOX green to DNA follows pseudo-first-order kinetics; thus we fit the increase in fluorescence signal observed in the second phase with a mono-exponential function of the form:

$$I(t) = I_F - (I_F - I_0)e^{-\frac{t}{\tau}} \quad (1)$$

where  $t$  is time,  $I(t)$  is the time-dependent fluorescence intensity signal,  $I_0$  is the baseline intensity,  $I_F$  is the final intensity, and  $\tau$  is the time constant. The data can be well fit by a single exponential function (Fig. 2b, red solid line), and  $1/\tau$  increases linearly with SYTOX green concentration (Fig. 2c), suggesting a bi-molecular reaction with a single rate-limiting kinetic step. The apparent association rate constant can be obtained from the slope of  $1/\tau$  as a function of concentration, and results in  $k_{\text{app}} = (1.5 \pm 0.5) \times 10^6 \text{ s}^{-1} \text{ M}^{-1}$ . It must be noted that in our experimental conditions this apparent association rate [i.e.,  $k_{\text{app}} \sim k_{\text{on}} \times (\text{SYTOX Green}) + k_{\text{off}}$ ] will give solely

an indirect estimation of the effective association rate ( $k_{\text{on}}$ ). However, this apparent rate is considerably slower than the diffusion rate for small molecules in solution (estimated at  $\sim 10^8 \text{ s}^{-1} \text{ M}^{-1}$  from the Smoluchowski equation) and could thus represent the rate of intercalation and conversion to a fluorescence-proficient complex after a fast diffusion-limited initial DNA association. The fluorescence signal from DNA-bound SYTOX green at equilibrium depends on ionic strength (Supplementary Fig. 1), consistent with an initial, diffusion-limited association step involving electrostatic interactions.

Next, we investigated the photobleaching rate of DNA-bound SYTOX green and compared it to that of DNA-bound YOYO-1 (both dyes at 40 nM, 1 W/cm<sup>2</sup>). In our conditions, YOYO-1 shows a small but noticeable photobleaching of the original intensity in a time scale of tens of seconds without recovery (Fig. 2d, bottom panel). The rate of YOYO-1 photobleaching can be considerably reduced in ROXS buffer (Reuter and Dryden 2010), but these conditions were often incompatible with PEG-coating due to condensation of DNA (Supplementary Fig. 2). In contrast, SYTOX green shows very little photobleaching as shown by time-lapse imaging over the same time period (Fig. 2d, top panel) and no DNA condensation was observed. Quantification of intensity signals from single DNA molecules at different times (Fig. 2e and Supplementary Fig. 3) shows that fluorescence from DNA-bound SYTOX green remains constant over relatively long periods of time ( $>40$  s) with  $>5\%$  loss in signal due to photobleaching, while fluorescence emission from DNA-bound YOYO-1 decreases  $<30\%$  in the same time period.

### Light-induced DNA cleavage by SYTOX green

The investigation of protein–DNA interactions by single-molecule fluorescence imaging requires the monitoring of fluorescence signals from both protein and DNA with a sufficiently high signal-to-noise ratio (SNR) for long periods of time ( $\sim$ min). High concentrations of DNA labeling agents, however, produce DNA damage through a photocleavage reaction that involves the generation of reactive

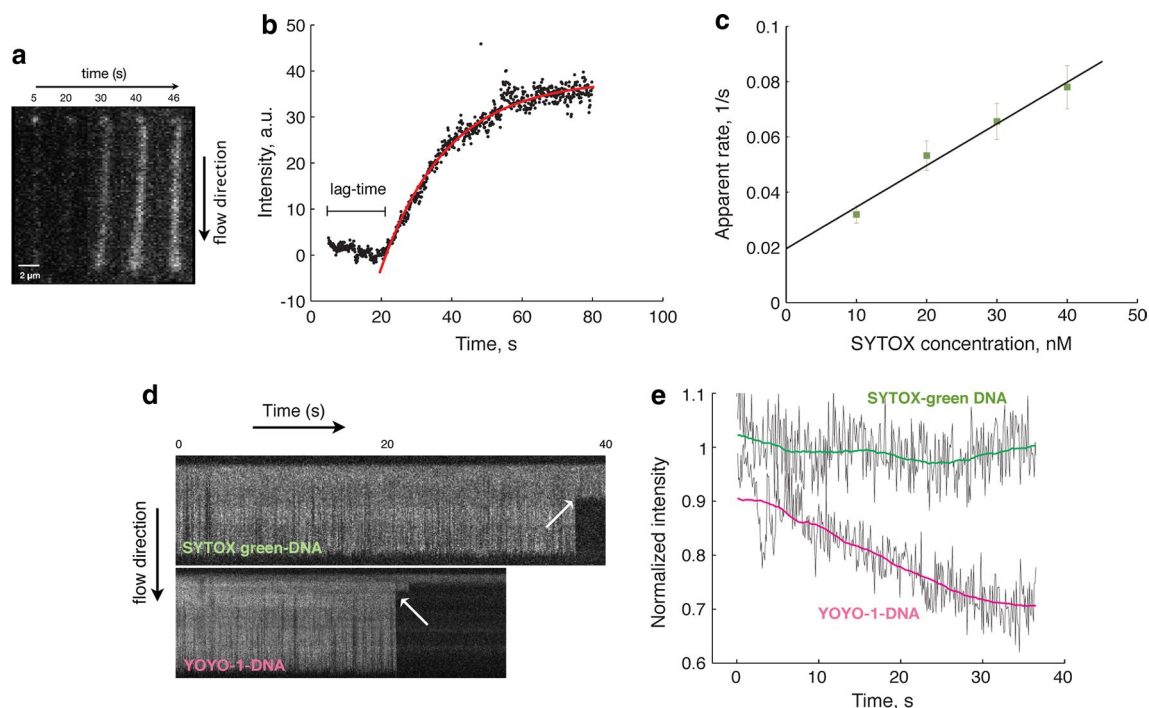


**Fig. 2** **a–c** Real-time imaging of SYTOX green binding kinetics. **a** Sequential images of single molecules of stretched  $\lambda$ -DNA after injection of 10 nM of SYTOX green. *White line* represents the *scale bar*. **b** SYTOX green fluorescence time-course. The mean integrated fluorescence intensity of a single DNA molecule was calculated and plotted vs. time (*black circles*). *Solid red line* represents the fitting of Eq. (1) to experimental data. The lag time before increase in fluorescence signal is indicated. **c** The inverse of the characteristic time ( $\tau$ ), obtained from the fitting of Eq. (1) to time courses, was plotted as a function of SYTOX green concentration (*green squares*). From the linear fitting to the experimental data (*solid black line*), the apparent association rate was calculated (see main text). **d** Photobleaching

properties of SYTOX green (*top panel*) and YOYO-1 (*bottom panel*). After equilibration, wide field images of stained samples were collected during 40 s at 100 ms per frame rate. Kymographs were constructed from images of single DNA molecules. *White arrows* indicate the breakage of the DNA tether. **e** YOYO-1 and SYTOX green photobleaching kinetics. The normalized mean fluorescence intensities (*grey lines*) of single DNA molecules stained with either dye are plotted as a function of time. *Solid lines* represent the mean fluorescence intensity averaged over five frames. DNA mean fluorescence intensity was background subtracted and normalized by the fluorescence signal at time zero

singlet oxygen and fluorophore radicals that attack DNA to produce ssb (Paillous and Vicendo 1993; Sangeetha Gowda et al. 2014). The accumulation of random ssb produces dsb that are observable in our experiments as shortening of DNA molecules (Fig. 2d). First, to characterize the degree of DNA damage by SYTOX green, we measured the percentage of broken DNA molecules at fixed imaging times (40 s) and a laser power of 5 W/cm<sup>2</sup>. The cumulative percentage of DNA molecules broken was plotted as a function of time (cumulative probability). These plots show that the number of broken DNA molecules increases considerably with SYTOX green concentration (Fig. 3a). Notably, a considerably larger number of DNA molecules break for YOYO-1-stained DNA even at concentrations four times lower than the maximum SYTOX green concentration employed (80 and 20 nM, respectively). At this laser power, at the lowest concentrations tested (10 nM), only ~10 % of DNA molecules break when stained with SYTOX green compared to 67 % for YOYO-1 staining. Furthermore, the

concentrations at which half the number of DNA molecules is degraded is eight times higher for SYTOX green than for YOYO-1 ( $c_{0.5}^{\text{YOYO-1}} = 5$  nM, and  $c_{0.5}^{\text{SYTOX}} = 40$  nM, Supplementary Fig. 4), consistent with a much lower degradation rate of DNA by SYTOX green. Next, we measured the average number of broken DNA molecules per unit time ( $n_b$ ) as a function of dye concentration (Fig. 3b). For both dyes,  $n_b$  increases linearly with concentration, with SYTOX green-stained molecules breaking consistently at a rate ~5 times lower than YOYO-1-stained DNA independently of dye concentration.

DNA photodamage depends linearly on the power used to excite fluorescent intercalators in its DNA-bound state (Tycon et al. 2012) and consequently affects the total time a single DNA molecule can be imaged without degradation. We characterized the DNA photodamage dependence on laser power at fixed SYTOX green and YOYO-1 concentrations (40 nM) by measuring the cumulative probability of DNA breakage and the number of DNA molecules broken

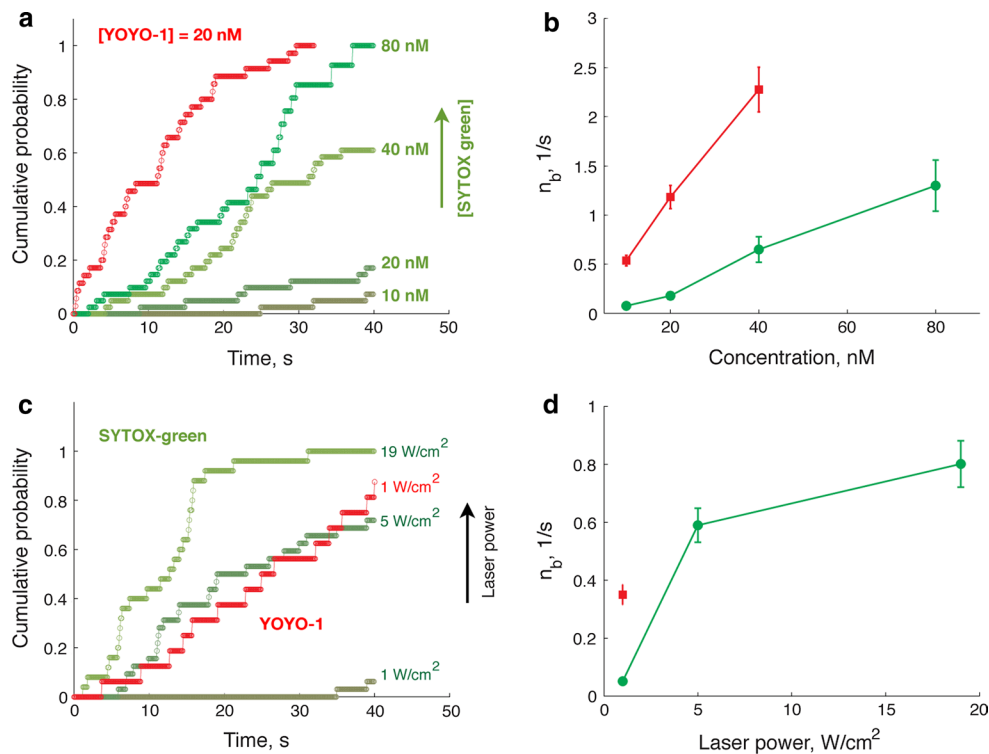


**Fig. 3** **a–b** Effect of dye concentration on production of dsb. **a** The cumulative probability of production of dsb is plotted as a function of time for different SYTOX green (*green curves*) concentrations and a fixed concentration of YOYO-1 (*red curve*). **b** The mean number of DNA molecules with dsb per second ( $n_b$ ) as a function of dye concentration is depicted (SYTOX green, *green circles*; YOYO-1, *red squares*). **c–d** Effect of laser power in the production of dsb. **c** Cumulative probability of production of a dsb is plotted as a function of time for SYTOX green and YOYO-1 (*green and red traces*,

respectively). **d** The mean number of dsb per second as a function of laser power is displayed (SYTOX green, *green circles*; YOYO-1, *red square*). Higher laser powers could not be explored for YOYO-1 due to the extremely fast breakage of DNA molecules. In panels **c** and **d**, both dye concentrations were fixed at 40 nM. Each *curve and data points* in panels **a–c** and **b–d**, respectively, were obtained from fields of view containing at least ~20–35 molecules. *Solid lines* in panels **b–d** are a guide to the eye

per second as a function of increasing excitation intensities (Fig. 3c, d). At low power densities (1 W/cm<sup>2</sup>), very low photo damage is observed for SYTOX green-stained DNA molecules over the entire imaging period (40 s). Under these conditions,  $n_b$  is extremely low (~0.07 molecules/s) and the signal-to-noise ratio (~6) remains relatively high (Supplementary Fig. 5). This allows imaging of single DNA molecules for minutes without detectable dsb or photobleaching at a reasonably high frame rate (10 Hz) and with a reasonably high signal-to-noise ratio (Supplementary Figs. 3, 5). At higher excitation powers, the SNR increases (Supplementary Fig. 5) but both the total number of broken DNA molecules (Fig. 3c) and the number of broken DNA molecules per unit time increase considerably (Fig. 3d). In contrast, we observe that even at the lowest power densities, most DNA molecules stained with 40 nM YOYO-1 degrade over the same imaging period and show a high rate of dsb (compare ~0.5 molecules/s for YOYO-1 vs. 0.07 molecules/s for SYTOX green, at 1 W/cm<sup>2</sup>) (Fig. 3c, d). At higher power densities, all YOYO-1-stained DNA

molecules break within a few seconds and could not be employed for this analysis.

### Mechanism of DNA binding by SYTOX green

SYTOX green has been described as a DNA staining agent that increases its fluorescence emission signal when bound to DNA, but it is not known whether the binding mechanism involves DNA intercalation. To address this question, we implemented a magnetic tweezers assay (Nollmann et al. 2007) to monitor whether DNA binding by SYTOX green changes the extension and mechanical properties of DNA. Briefly, ~14.7-kbp DNA molecules (4.98 μm in length) are attached to a glass coverslip and a magnetic bead by biotin-streptavidin and digoxigenin/anti-digoxigenin interactions (see “Materials and methods”). Tethers used in these experiments contained specifically engineered DNA nicks and therefore were unable to sustain topological constraints. A permanent magnet is used to stretch DNA in the optical axis ( $z$ ), and different tensions are applied by

varying the position of the magnets relative to the coverslip along the  $z$  direction (Fig. 4a). Real-time 3D tracking of the bead is performed through image analysis as described elsewhere, with changes in the height representing changes in DNA extension (Nollmann et al. 2007).

In order to determine if intercalation of SYTOX green changes the mechanical properties of DNA, force-extension curves (FEC) of single DNA molecules were measured at saturating concentration of SYTOX green (1  $\mu\text{M}$ , see below equilibrium binding) by calculating the end-to-end extension of each DNA molecule as a function of force. In the absence or presence of SYTOX green, the

represents the number of SYTOX green binding sites per base pair, and  $K_{\text{Sytox}}^{n_H}$  the apparent association constant for the SYTOX green–DNA complex. SYTOX green binds to DNA with high affinity ( $K_d = 1/K_{\text{Sytox}}^{n_H} = 40$  nM) and in a cooperative manner ( $n_H \sim 2$ ). From the average number of occupied sites at saturation ( $0.27 \pm 0.01$ ), we can calculate a minimal size of SYTOX green binding site of  $3.7 \pm 0.1$  bp.

To further evaluate the DNA–SYTOX green binding behavior, we employed the neighbor exclusion model for cooperative systems developed by McGhee and von Hippel (McGhee and von Hippel 1974) (Table 1):

$$\frac{\langle n \rangle}{[\text{Sytox}]_f} = K_s(1 - l\langle n \rangle) \left[ \frac{(2\omega - 1)(1 - l\langle n \rangle) + \langle n \rangle - R}{(2\omega - 1)(1 - l\langle n \rangle)} \right]^{l-1} \left[ \frac{1 - (l+1)\langle n \rangle + R}{2(1 - l\langle n \rangle)} \right]^2 \quad (3)$$

$$R = \left\{ [1 - (l+1)\langle n \rangle]^2 + 4\omega\langle n \rangle(1 - l\langle n \rangle) \right\}^{1/2}$$

force-extension curves can be well fit by a worm-like chain model (Bustamante et al. 1994) (Fig. 4b). In the absence of SYTOX green, the persistence length ( $L_p$ ) is  $50 \pm 5$  nm and the full extension  $4.9 \pm 0.1$   $\mu\text{m}$ , consistent with the expected crystallographic length of the molecule (4.99  $\mu\text{m}$ ) and literature values for the persistence length of DNA in 10 mM phosphate saline buffer ( $51 \pm 2$  nm) (Bouchiat et al. 1999). In the presence of saturating amounts of SYTOX green, the length of the molecule increased to  $7.1 \pm 0.1$   $\mu\text{m}$ , indicating a 43 % increase in length, while the persistence length remained at  $52 \pm 5$  nm. This increase in DNA length strongly suggests that SYTOX green intercalates between consecutive base pairs (Coury et al. 1996; Sischka et al. 2005) while it does not affect the elastic properties of DNA.

To further characterize the binding mechanism of SYTOX green, we performed bulk fluorescence measurements in which we measured the equilibrium fluorescence signal increase as a function of SYTOX green concentration. Our results show that the average number of occupied sites, representing the average number of dye molecules per base pair, increases as a function of free dye concentration (Fig. 4c). The fluorescence signal increases ~1500-fold upon intercalation, and binding saturation was achieved with SYTOX green concentrations above 800 nM. Different binding mechanisms were evaluated (single and multiple independent sites assuming identical quantum yields) and the best fit was achieved when using a Hill equation (Table 1):

$$\langle n \rangle = \frac{N[\text{Sytox}]_f^{n_H}}{\frac{1}{K_{\text{Sytox}}^{n_H}} + [\text{Sytox}]_f^{n_H}} \quad (2)$$

where  $n_H$  represents an empirical coefficient that takes into account the non-hyperbolic behavior (Hill coefficient),  $N$

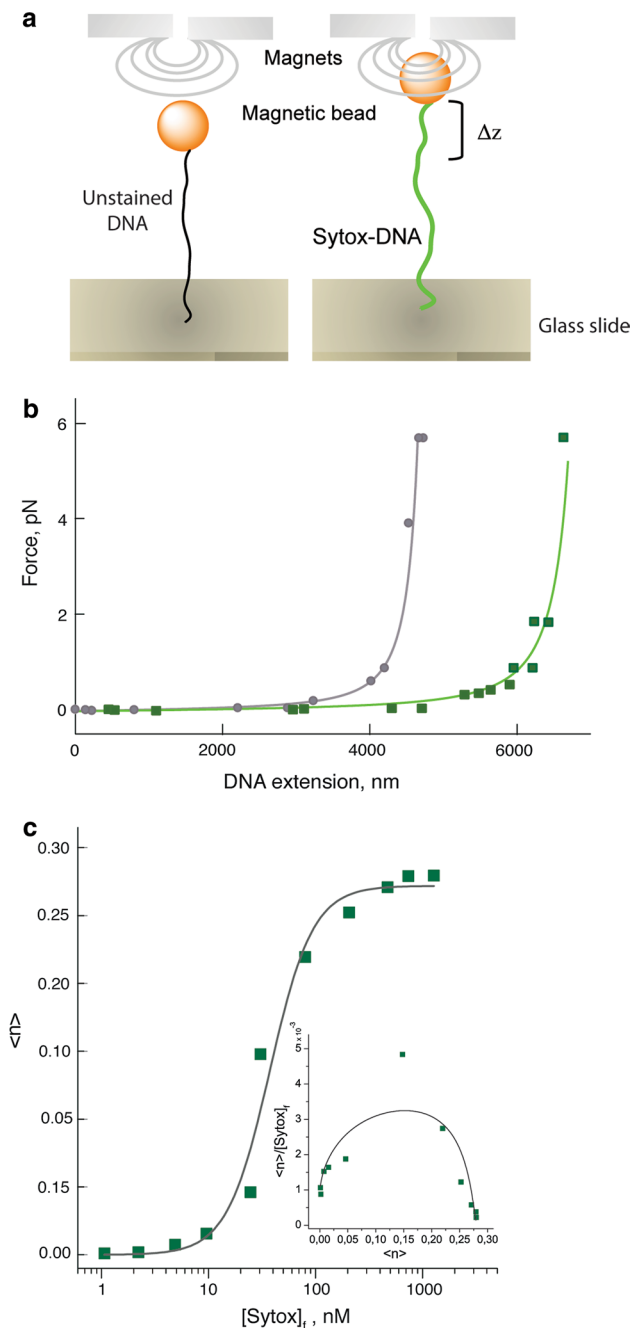
where  $l$  represents the binding site size of SYTOX green (in units of nucleotide residues or base pairs);  $K_s$  the intrinsic binding constant and  $\omega$  the cooperativity parameter that specifies the relative affinity of an incoming ligand for a contiguous occupied site as opposed to an isolated binding site (Kowalczykowski et al. 1986). When re-plotting  $\langle n \rangle / [\text{Sytox}]_f$  as a function of  $\langle n \rangle$ , the Scatchard plot shows positive slopes at low binding ratios (inset Fig. 4c) confirming the existence of positive cooperativity (Chaires 2001) as suggested by the Hill model. Fitting of Eq. (3) to the experimental data yielded a binding site size of 3.5 bp/dye in good agreement with that obtained by the Hill model (3.7 bp/dye). The positive value of  $\omega$  (24.6) is consistent with cooperative binding, while the product of the cooperativity parameter and  $K_s$  allows for the calculation of a total apparent affinity of  $2 \times 10^7$   $\text{M}^{-1}$  ( $K_d \sim 48$  nM), in very good agreement with the values obtained by the Hill approach.

From our measurements, the DNA elongation per intercalated SYTOX green molecule can be estimated as  $[z(c_{\text{sat}}) - z_0] \times I/n_{\text{bp}} = (2.16 \mu\text{m}) \times 3.5 \text{ bp}/14.7 \times 10^3 \text{ bp} \sim 0.51$  nm/dye, where  $[z(c_{\text{sat}}) - z_0]$  is the fractional DNA length increase at saturation dye concentration ( $c_{\text{sat}} = 800$  nM),  $I$  is the binding site size in base pairs, and  $n_{\text{bp}}$  is the total number of base pairs in DNA. Thus, the intercalation of a single SYTOX green molecule increases the average distance between base pairs by  $\sim 0.17$  nm/dye.

## Discussion

Here, we use single-molecule fluorescence and manipulation to investigate the binding mechanism and fluorescence emission properties of the DNA labeling agent SYTOX





green. SYTOX green has a high affinity for DNA ( $K_d = 40$  nM) and its apparent association rate in TIRF imaging conditions is relatively fast ( $1.5 \times 10^6 \text{ M}^{-1} \text{ s}^{-1}$ ). At the dye concentration used in this study, the diffusion-limited association time constant is expected to be  $\sim 0.1$  s, much faster than the time constants measured (10–50 s). Thus, the production of a fluorescence-proficient SYTOX green–DNA complex could involve at least two steps: (1) rapid association to DNA by three-dimensional diffusion, which most probably involves binding of the dye to the phosphate chain primarily through electrostatic interactions, and (2) conversion

**Fig. 4** **a** Scheme depicting the magnetic tweezers setup used. A double-stranded DNA molecule (black line) is tethered between a glass slide and a magnetic bead. Tension on the DNA molecule is introduced using magnets and the DNA extension change after injection of SYTOX green (right panel) is monitored by the change in height ( $\Delta z$ ) of the magnetic bead. **b** SYTOX green does not affect the elasticity of DNA. Force-extension curves (FEC) for bare DNA (grey circles) and for SYTOX green-bound DNA (green squares, concentration = 1  $\mu\text{M}$ ). **c** SYTOX green-DNA equilibrium fluorescence binding isotherm. The average number of occupied binding sites (or dye molecules per base pair) and the free ligand concentration were calculated using Eqs. M2 and M3 (see “Materials and methods”). The continuous line is the graphical representation of Eq. (2) with best fitting parameter values  $N = 0.27 \pm 0.01$ ,  $K_{\text{Sytox}}^{\text{MH}} = (2.5 \pm 0.4) \times 10^7 \text{ M}^{-1}$  and  $n_{\text{H}} = 2.1 \pm 0.5$ . Inset shows the Scatchard representation of the SYTOX green-DNA binding isotherm. Solid line shows the graphical representation of the McGhee–von Hippel neighbor exclusion model with added ligand–ligand cooperativity (Eq. 3) with the best fitting parameters described in the main text

into a fluorescence-proficient complex that involves DNA intercalation. The formation of an intercalated SYTOX green–DNA complex requires large conformational transitions occurring simultaneously both in DNA and the dye, thereby providing a rationale for the existence of a transient non-fluorescent complex and a sequential mechanism with a slow step. A second and alternative hypothesis for the reduced rate of the second step is that only dye molecules having a favorable orientation (i.e., parallel to the DNA bases) can bind stably and therefore only a fraction of the total collisions of SYTOX green with DNA results in intercalated/fluorescent complexes. Binding mechanisms involving two states were proposed in the past for bis-intercalators (Murade et al. 2009), and more recently for mono-intercalators (YO-1) (Paik and Perkins 2012).

Single-molecule DNA imaging requires the ability to detect DNA for long periods of time, a need that is counteracted by both photobleaching and photo-damage. Bis-intercalators such as YOYO-1 were proposed to photobleach by a mechanism that involves quenching of the dye fluorescence by modified DNA bases, and thus the use of conventional ROS scavengers did not considerably reduce the degree of photobleaching (Kanony et al. 2001). In particular, photobleaching becomes acute in single-molecule experiments as it is not possible to restore the fluorescence of intercalator-saturated DNA samples by re-staining after photobleaching, probably due to the slow off-rate of bis-intercalators (Baumann et al. 1997; Kanony et al. 2001). Interestingly, our experiments have shown a lower degree of effective photobleaching (i.e., the combination of ‘true’ photobleaching and binding dynamics) for SYTOX green than for YOYO-1-stained DNA. This phenomenon can be explained by the faster dynamics of SYTOX green–DNA association ( $\tau \sim 10$  s at 40 nM SYTOX green) and dissociation times [ $1/k_{\text{off}} = 1/(k_{\text{app}} \times K_d) \sim 15$  s] with respect to the intrinsic rate of SYTOX green photobleaching. These

dynamics are such that DNA-bound SYTOX green molecules can rapidly exchange with free, fluorescent-proficient molecules from bulk solution, leading to a stationary state in which DNA is constantly replenished with unbleached molecules and thus conserves its fluorescence signal for long periods of time.

The damage produced by the excitation of fluorescent DNA intercalators has been extensively investigated. Monomeric and dimeric dyes degrade DNA not by directly producing double-strand breaks but rather by the accumulation of single-strand breaks that eventually produce dsDNA cleavage. Both externally bound and intercalated dyes were shown to trigger ssb by mechanisms that are singlet oxygen-dependent or independent (Akerman and Tuite 1996). The rate of dsb by bis-intercalators was shown to be considerably higher than that of mono-intercalators due to their slower dissociation rate, which allows them to repeatedly attack the phosphoribose backbone ~5–6 bp away from their binding site (Akerman and Tuite 1996). Photocleavage by intercalated dyes can be inhibited by adding ROS scavenging reagents (such as  $\beta$ -mercaptoethanol, or glucose oxidase/catalase), but particularly for YOYO-1 these reagents trigger DNA condensation (Kuyper et al. 2003) and promote non-specific interactions with the passivated surface (Supplementary Fig. 2) due to local solution acidification induced by the oxygen scavenging system (Shi et al. 2010). To avoid the latter, YOYO-1-stained DNA can be imaged in the presence of DTT (but in absence of other ROS scavengers). However, this leads to important DNA cleavage rates due to the accumulation of a large number of ssb that become apparent in the microscope in the form of an observable dsb [typically assumed to be ~20–70 ssb per dsb as observed from agarose-gels electrophoresis measurements (Akerman and Tuite 1996; Krisch et al. 1991; Prise et al. 2000)]. In addition to reducing imaging time, these effects could have an effect on the properties of DNA, and the binding and movement of proteins on it. In contrast, our results show that the rates of dsb by SYTOX green in the absence of ROS scavengers are at least four times lower than those of YOYO-1 without any DNA condensation, making it a better-suited dye for single-molecule microscopy, especially for methods that require DNA immobilization onto a passivated surface, such as TIRFM. These results are consistent with the fivefold difference in the rates of dsb previously observed between mono-intercalators (YO-1) and YOYO-1 (Akerman and Tuite 1996), and suggest that dsb by SYTOX green does not involve repeated attack of the phosphoribose backbone close (~5–6 bp) to their binding site as observed for bis-intercalators.

Next, we used magnetic tweezers and ensemble binding assays to investigate the mechanism of DNA binding of SYTOX green. First, we showed that at equilibrium SYTOX green occupies a minimum of ~3.5 bp. These

values are in agreement with those reported for other monointercalators, such as ethidium bromide (~2.4–3 bp) (Vladescu et al. 2007), and YO-1 (~4 bp) (Murade et al. 2009), or for bis-intercalators such as YOYO-1 (3.2 bp) (Günther et al. 2010) or triostin A (4 bp) (Kleimann et al. 2009). Secondly, we showed that upon intercalation of SYTOX green, the extension of the DNA molecule increases by ~43 %, which is consistent with fractional elongations reported for other intercalators (17–47 %) (Chaurasiya et al. 2010). By combining the binding site size and the fractional elongation, we can calculate that intercalation of SYTOX green increases the DNA length by  $0.51 \text{ nm/dye} = 1.5 \text{ bp/dye}$ . This elongation of DNA upon intercalation is larger than that reported for other monointercalators, such as ethidium bromide (0.27–0.34 nm/dye) (Chaurasiya et al. 2010; Coury et al. 1996; Sischka et al. 2005; Vladescu et al. 2007) or YO-1 (0.32 nm/dye) (Chaurasiya et al. 2010; Murade et al. 2009), and similar to that reported for bis-intercalators such as YOYO-1 (0.54 nm/dye) (Günther et al. 2010) or triostin A (~0.44 nm/dye) (Kleimann et al. 2009). Further information on the specific chemical structure and valence of SYTOX green will be needed to explain this discrepancy.

We found that intercalation by SYTOX green does not modify the persistence length of the DNA molecule. Previous optical tweezers studies using high-force stretching (~50 pN) and high salt concentrations (~150 mM) have reported a ~25 % reduction in the persistence length upon intercalation of monomeric dyes such as ethidium bromide (Sischka et al. 2005) or YO-1 (Murade et al. 2009; Sischka et al. 2005) and even a larger decrease for YOYO-1 (Murade et al. 2009; Sischka et al. 2005). The high salt concentrations and high DNA stretching forces used in those studies led to a slow, out-of-equilibrium incorporation of dye during stretching, thus changing the binding equilibrium and reducing the apparent persistence length (Günther et al. 2010). In contrast, and similarly to our results, constant-force magnetic tweezers experiments performed at low stretching forces (<10 pN) and low ionic strength (18 mM sodium ions) showed no change in the persistence length of YOYO-1 upon intercalation (Günther et al. 2010). In that study, two hypotheses were introduced to explain this result. The first invoked a compensation between two effects: (1) a decrease in persistence length induced by reduction in electrostatic inter-segment repulsion upon YOYO-1 binding leading to increased DNA flexibility, and (2) an increase in persistence length due to additional stiffening induced by bis-intercalation. The second hypothesis proposed that the electrostatic changes induced by YOYO-1 binding to DNA do not influence its persistence length, as the persistence length of bare DNA is mostly independent of ionic strength (at monosalt concentrations larger than 10 mM) (Baumann et al. 1997). Our

results do not support the first hypothesis, which requires the proposed stiffening provided by bis-intercalators, and is fully consistent with the second model by which charge compensation upon complexation of DNA intercalators such as SYTOX green do not affect the mechanics of DNA.

Previous binding studies of DNA labeling agents have used relatively high concentrations (i.e., in the  $\mu\text{M}$  range) of bound intercalator and in non-equilibrium conditions (e.g., electrophoresis gels), concealing perhaps important details of the binding mechanism. Here, by employing low concentrations of SYTOX green, we show the existence of positive cooperativity in its binding to DNA. Positive cooperativity has been previously observed for several DNA intercalating binding drugs (e.g., m-AMSA, actinomycin, anthracenedione (Elmore et al. 1988). Additionally, by employing molecular dynamics simulations including entropic effects, Trieb et al. (2004) showed that the Gibbs free energy necessary to form a single intercalation site in DNA by a monointercalator is 32.3 kcal/mol, whereas for the formation of two sites it is 54.4 kcal/mol, indicating that the formation of a DNA cavity costs less energy, if a second intercalator joins the first. The absence of the molecular structure of SYTOX green makes it difficult to speculate on the physicochemical properties that dictate the cooperativity mechanism (e.g., stabilizing charge distribution between base pairs).

## Conclusions

Single-molecule microscopy methods allow obtaining mechanistic insight of protein–DNA interactions that cannot be normally observed by ensemble methods. These approaches require, in most cases, direct labeling of DNA and proteins with fluorescent compounds that may affect DNA structure and mechanical properties, enzymes activities, and introduce light-induced damage to the biomolecules of interest. Finding new fluorescent compounds that allow optimal imaging conditions while introducing minimal perturbations to the system under study is of outmost importance.

In this work, we studied a fluorescent dye, SYTOX green, which allows for a significant simplification and shortening of the DNA staining protocol, including *in situ* labeling, while improving imaging conditions without affecting DNA mechanical properties. Specifically, we determine that SYTOX green: (1) binds DNA rapidly in a process that involves electrostatic interactions; (2) has a good signal-to-noise ratio, even at low concentrations, (3) shows a low photobleaching rate; (4) induces fourfold lower light-induced DNA degradation than that observed for bis-intercalators, such as YOYO-1; and (5) binds DNA by intercalating cooperatively with a 3.5-bp binding site size, and an increase in DNA length upon binding of 43 %.

Our results suggest that SYTOX green represents a valuable alternative to conventional fluorophores employed for single-molecule imaging. The rapid binding kinetics, high photo-stability, low DNA-damaging rates, and mild effect over the mechanical properties of DNA make SYTOX green a rather appealing and advantageous choice for single-molecule and single-cell microscopy and other methods requiring sensitive detection and low perturbation of DNA. Our characterization of the photo-damage and mechanical properties of SYTOX green-complexed DNA will be of use for the interpretation of single-molecule experiments using SYTOX green as an intercalating dye. Further studies should confirm if the advantages we found for SYTOX green could be extrapolated to other molecules of the SYTOX family spanning the visible spectrum.

**Acknowledgments** We acknowledge Catherine Royer for critical reading of the manuscript and Stephanie Dejardin for the preparation of DNA substrates. Fluorescence anisotropy and TIRF experiments were performed at the Biophysics facility of the Centre de Biochimie Structurale (CBS) funded by the Plate-forme Intégrée de Biologie Structurale (IBISA) and the France-BioImaging infrastructure supported by the French National Research Agency (ANR-10-INSB-04, “Investments for the future”). This work was supported by the Agence Nationale de la Recherche (ANR-2010-BLAN-1525-01, and ANR-2010-BLAN-1221-01), and the Human Frontiers Science Program through a Career Development Award (M.N.).

## References

- Akerman B, Tuite E (1996) Single- and double-strand photocleavage of DNA by YO, YOYO and TOTO. *Nucleic Acids Res* 24:1080–1090
- Amitani I, Baskin RJ, Kowalczykowski SC (2006) Visualization of Rad54, a chromatin remodeling protein, translocating on single DNA molecules. *Mol Cell* 23:143–148
- Baumann CG, Smith SB, Bloomfield VA, Bustamante C (1997) Ionic effects on the elasticity of single DNA molecules. *Proc Natl Acad Sci USA* 94:6185–6190
- Bianco PR, Brewer LR, Corzett M, Balhorn R, Yeh Y, Kowalczykowski SC, Baskin RJ (2001) Processive translocation and DNA unwinding by individual RecBCD enzyme molecules. *Nature* 409:374–378
- Blainey PC, van Oijen AM, Banerjee A, Verdine GL, Xie XS (2006) A base-excision DNA-repair protein finds intrahelical lesion bases by fast sliding in contact with DNA. *Proc Natl Acad Sci USA* 103:5752–5757
- Bouchiat C, Wang MD, Allemand J, Strick T, Block SM, Croquette V (1999) Estimating the persistence length of a worm-like chain molecule from force-extension measurements. *Biophys J* 76:409–413
- Bustamante C, Marko JF, Siggia ED, Smith S (1994) Entropic elasticity of lambda-phage DNA. *Science* 265:1599–1600
- Cadet J, Douki T, Gasparutto D, Ravanat JL (2003) Oxidative damage to DNA: formation, measurement and biochemical features. *Mutat Res* 531:5–23
- Carlsson C, Jonsson M, Akerman B (1995) Double bands in DNA gel electrophoresis caused by bis-intercalating dyes. *Nucleic Acids Res* 23:2413–2420
- Chaires JB (2001) Analysis and interpretation of ligand-DNA binding isotherms. *Methods Enzymol* 340:3–22

- Chaurasiya KR, Paramanathan T, McCauley MJ, Williams MC (2010) Biophysical characterization of DNA binding from single molecule force measurements. *Phys Life Rev* 7:299–341
- Colmenarejo G, Bárcena M, Carmen Gutiérrez-Alonso M, Montero F, Orellana G (1995) DNA photocleavage by novel intercalating 6-(2-pyridinium)phenanthridinium viologens. *FEBS Lett* 374:426–428
- Coury JE, McFail-Isom L, Williams LD, Bottomley LA (1996) A novel assay for drug-DNA binding mode, affinity, and exclusion number: scanning force microscopy. *Proc Natl Acad Sci USA* 93:12283–12286
- Daniel E, Weber G (1966) Cooperative effects in binding by bovine serum albumin. I. The binding of 1-anilino-8-naphthalenesulfonate. *Fluorim Titrations Biochem* 5:1893–1900
- Elmore RH, Wadkins RM, Graves DE (1988) Cooperative binding of m-AMSA to nucleic acids. *Nucleic Acids Res* 16:9707–9719
- Günther K, Mertig M, Seidel R (2010) Mechanical and structural properties of YOYO-1 complexed DNA. *Nucleic Acids Res* 38:6526–6532
- Gurrieri S, Wells KS, Johnson ID, Bustamante C (1997) Direct visualization of individual DNA molecules by fluorescence microscopy: characterization of the factors affecting signal/background and optimization of imaging conditions using YOYO. *Anal Biochem* 249:44–53
- Hamdan S, Loparo J, Takahashi M, Richardson C, Van Oijen A (2009) Dynamics of DNA replication loops reveal temporal control of lagging-strand synthesis. *Nature* 457:336–339
- Hurley LH (2002) DNA and its associated processes as targets for cancer therapy. *Nat Rev Cancer* 2:188–200
- Kanony C, Akerman B, Tuite E (2001) Photobleaching of asymmetric cyanines used for fluorescence imaging of single DNA molecules. *J Am Chem Soc* 123:7985–7995
- Kleimann C, Sischka A, Spiering A, Tönsing K, Sewald N, Diederichsen U, Anselmetti D (2009) Binding kinetics of bisintercalator Triostin A with optical tweezers force mechanics. *Biophys J* 97:2780–2784
- Kowalczykowski SC, Paul LS, Lonberg N, Newport JW, McSwiggen JA, von Hippel PH (1986) Cooperative and noncooperative binding of protein ligands to nucleic acid lattices: experimental approaches to the determination of thermodynamic parameters. *Biochemistry* 25:1226–1240
- Krisch RE, Flick MB, Trumbore CN (1991) Radiation chemical mechanisms of single- and double-strand break formation in irradiated SV40 DNA. *Radiat Res* 126:251–259
- Kuyper CL, Brewood GP, Chiu DT (2003) Initiating conformation transitions of individual YOYO-intercalated DNA molecules with optical trapping. *Nano Lett* 3:1387–1389
- Lerman LS (1961) Structural considerations in the interaction of DNA and acridines. *J Mol Biol* 3:18–30
- Loparo JJ, Kulczyk AW, Richardson CC, van Oijen AM (2011) Simultaneous single-molecule measurements of phage T7 replisome composition and function reveal the mechanism of polymerase exchange. *Proc Natl Acad Sci USA* 108:3584–3589
- Marko JF, Siggia ED (1994) Bending and twisting elasticity of DNA. *Macromolecules* 27:981–988
- McGhee JD, von Hippel PH (1974) Theoretical aspects of DNA-protein interactions: co-operative and non-co-operative binding of large ligands to a one-dimensional homogeneous lattice. *J Mol Biol* 86:469–489
- Murade CU, Subramaniam V, Otto C, Bennink ML (2009) Interaction of oxazole yellow dyes with DNA studied with hybrid optical tweezers and fluorescence microscopy. *Biophys J* 97:835–843
- Nollmann M et al (2007) Multiple modes of *Escherichia coli* DNA gyrase activity revealed by force and torque. *Nat Struct Mol Biol* 14:264–271
- Paik DH, Perkins TT (2012) Dynamics and multiple stable binding modes of DNA intercalators revealed by single-molecule force spectroscopy. *Angew Chem Int Ed Engl* 51:1811–1815
- Pailous N, Vicendo P (1993) Mechanisms of photosensitized DNA cleavage. *J Photochem Photobiol B Biol* 20:203–209
- Petty JT, Bordelon JA, Robertson ME (2000) Thermodynamic characterization of the association of cyanine dyes with DNA. *J Phys Chem B* 104:7221–7227
- Prise KM, Folkard M, Michael BD, Vojnovic B, Brocklehurst B, Hopkirk A, Munro IH (2000) Critical energies for SSB and DSB induction in plasmid DNA by low-energy photons: action spectra for strand-break induction in plasmid DNA irradiated in vacuum. *Int J Rad. Biol* 76:881–890
- Ptacin JL, Nollmann M, Becker EC, Cozzarelli NR, Pogliano K, Bustamante C (2008) Sequence-directed DNA export guides chromosome translocation during sporulation in *Bacillus subtilis*. *Nat Struct Mol Biol* 15:485–493
- Reuter M, Dryden DTF (2010) The kinetics of YOYO-1 intercalation into single molecules of double-stranded DNA. *Biochem Biophys Res Commun* 403:225–229
- Roth BL, Poot M, Yue ST, Millard PJ (1997) Bacterial viability and antibiotic susceptibility testing with SYTOX green nucleic acid stain. *Appl Environ Microbiol* 63:2421–2431
- Sangeetha Gowda KR, Blessy Baby M, Sudhamani CN, Bhojya Naik HS (2014) Mechanism of DNA binding and cleavage. *Biomed Biotechnol* 2:1–9
- Shi X, Lim J, Ha T (2010) Acidification of the oxygen scavenging system in single-molecule fluorescence studies: in situ sensing with a ratiometric dual-emission probe. *Anal Chem* 82:6132–6138
- Sischka A, Tönsing K, Eckel R, Wilking SD, Sewald N, Ros R, Anselmetti D (2005) Molecular mechanisms and kinetics between DNA and DNA binding ligands. *Biophys J* 88:404–411
- Stone MD, Bryant Z, Crisona NJ, Smith SB, Vologodskii A, Bustamante C, Cozzarelli NR (2003) Chirality sensing by *Escherichia coli* topoisomerase IV and the mechanism of type II topoisomerases. *Proc Natl Acad Sci USA* 100:8654–8659
- Tanner N, Loparo J, Hamdan S, Jergic S, Dixon N, Van Oijen A (2009) Real-time single-molecule observation of rolling-circle DNA replication. *Nucleic Acids Res* 37:27
- Trieb M, Rauch C, Wibowo FR, Wellenzohn B, Liedl KR (2004) Cooperative effects on the formation of intercalation sites. *Nucleic Acids Res* 32:4696–4703
- Tycon MA, Dial CF, Faison K, Melvin W, Fecko CJ (2012) Quantification of dye-mediated photodamage during single-molecule DNA imaging. *Anal Biochem* 426:13–21
- van Mameren J, Peterman EJ, Wuite GJ (2008) See me, feel me: methods to concurrently visualize and manipulate single DNA molecules and associated proteins. *Nucleic Acids Res* 36:4381–4389
- Vladescu ID, McCauley MJ, Nunez ME, Rouzina I, Williams MC (2007) Quantifying force-dependent and zero-force DNA intercalation by single-molecule stretching. *Nat Methods* 4:517–522
- Yan X, Habbersett RC, Cordek JM, Nolan JP, Yoshida TM, Jett JH, Marrone BL (2000) Development of a mechanism-based, DNA staining protocol using SYTOX orange nucleic acid stain and DNA fragment sizing flow cytometry. *Anal Biochem* 286:138–148
- Yu H-J et al (2009) Synthesis, DNA-binding and photocleavage studies of ruthenium complexes [Ru(bpy)<sub>2</sub>(mitatp)]<sup>2+</sup> and [Ru(bpy)<sub>2</sub>(nitatp)]<sup>2+</sup>. *J Inorg Biochem* 103:881–890